

Mater. Res. Soc. Symp. Proc. Vol. 1417 © 2012 Materials Research Society
DOI: 10.1557/opl.2012.1014

ERRATUM

Microencapsulation of Liquid Cyanoacrylate via In Situ Polymerization for Self-healing Bone Cement Application – **ERRATUM**

Vineela D. Gandham, Alice B.W. Brochu, and William M. Reichert
doi:10.1557/opl.2012.1014, Published by Materials Research Society, 25th May 2012.

The article by Gandham et al. was still in the process of revision when it was erroneously published. Materials Research Society and Cambridge University Press apologize to the authors for this oversight. The final, accepted, and correct version of the article follows this notice.

REFERENCES

1. Vineela D. Gandham, Alice B.W. Brochu, and William M. Reichert, Mater. Res. Soc. Symp. Proc. **1417**, MRSF11-1417-KK01-06. doi:10.1557/opl.2012.1014 (2012).

Microencapsulation of Liquid Cyanoacrylate via *In situ* Polymerization for Self-Healing Bone Cement Application

Vineela D. Gandham¹, Alice B.W. Brochu^{1,2}, William M. Reichert^{1,2}

¹Department of Biomedical Engineering, Duke University, Durham, NC 27708-0281, U.S.A.

²Center for Biomolecular and Tissue Engineering, Duke University, Durham, NC 27708-0271, U.S.A.

ABSTRACT

Structural polymers are susceptible to accumulated damage in the form of internal microcracks that propagate through the material, resulting in mechanical failure. Self-healing approaches offer a solution to repair these damages automatically. The first generation self-healing material system includes a microencapsulated healing agent within a catalyst-embedded matrix. Propagating microcracks rupture the microcapsules, releasing the liquid healing agent into the damaged region. Catalyst-triggered polymerization of the released healing agent repairs the damage. This research focuses on a similar approach for addressing “damage accumulation failure” of poly(methyl methacrylate) (PMMA) bone cement caused by microcrack initiation and propagation. In this study, polyurethane (PU) microcapsules containing a tissue adhesive, 2-octylcyanoacrylate (OCA) were synthesized using *in situ* interfacial polymerization of toluene-2,4-diisocyanate (TDI) and polyethylene glycol 200 (PEG 200) through an oil-in-oil-in-water microemulsion (o/o/w). The process was optimized by studying different combinations of organic solvents, surfactants, temperatures, agitation rates, pH, and reaction times and their effects on microencapsulation were observed. Microcapsule surface morphology, size, shell thickness, encapsulated OCA viability, thermal degradation, and chemical structure of the microcapsule shell were evaluated using a stereoscope, scanning electron microscopy (SEM), thermogravimetric analysis (TGA), and Fourier transform infrared spectroscopy (FT-IR).

INTRODUCTION

Through the pioneering efforts of Charnley as reviewed by Kindt-Larsen *et al.*, [1] poly(methyl methacrylate) (PMMA) bone cement emerged as one of the promising biomaterials in orthopedics. PMMA acts as a space-filler, holding the stem of an artificial joint replacement against the native bony tissue. However, these replacements tend to fail mostly due to aseptic loosening of the construct or through immunological rejections. Jasty *et al.* [2] have shown that orthopedic implants mostly fail due to the “damage accumulation failure” of the bone cement during which numerous microcracks initiate and propagate, leading to loosening and subsequent failure of the prosthesis. Evidence of damage accumulation and microcrack initiation under dynamic loading in cement mantle was observed by Culleton *et al.* [3] and Topoleski *et al.* [4]. Cracks ranging in length from 40 μm to 2 mm were observed in bone cement mantles retrieved *post-mortem*. However, only microcracks greater than 300 μm in length were found to have the potential to grow to critical length and cause implant failure [2,5]. Bone cement is a brittle material with weak tensile and shear strengths, but high compressive strength. The average

values of tensile strength of the bone cement range from 21.7 to 34.8 MPa, while the compressive strength ranges from 64 to 103 MPa and the Young's modulus ranges from 3150 to 5050 MPa [6]. Loosening of cemented implants is usually caused by mechanical failure of the PMMA bone cement under cyclic loading [7]. Previous studies have addressed these problems by modifying the cement formulation through the addition of cross linking agents [8,9], increasing tensile strength and fracture toughness by reinforcing with metallic wires, or incorporating covalently connected SiO₂ glass networks to prevent bone cement failure [10-12]. However, limited success was seen in resolving "damage accumulation failure" of the cemented implants.

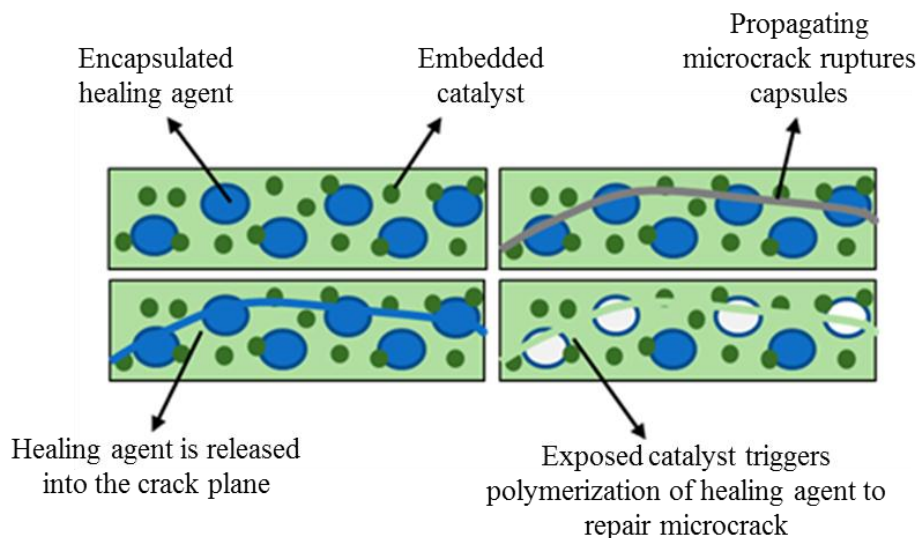


Figure 1: Mechanism of self-healing using an embedded microcapsule system

In this study, a self-healing bone cement approach where microcracks can be autonomously healed, preventing "damage accumulation failure" of the cement by arresting further propagation of the cracks is proposed [13]. Self-healing materials are designed to sense failure and respond to the damage in an autonomous fashion to restore material structural function. The design approach used in this work was adopted from an existing self-healing system pioneered by White *et al.* [14] that includes a matrix co-embedded with microcapsules containing an encapsulated healing agent and a solid chemical catalyst. Microcracks propagating through the matrix rupture the microcapsules, releasing healing agent into the cracked region, leading to damage repair by its polymerization in the presence of a catalyst [15] (Figure 1). Microcapsules are small particles with diameters ranging from micrometers to millimeters and consist of a core material encapsulated within a polymeric membrane [16-18]. This embedded microcapsule approach offers remarkable potential for practical applications [14,15,19]; Sottos *et al.* [15] reported 75% healing efficiency in a self-healing epoxy polymer embedded with microencapsulated dicyclopentadiene and Grubb's catalyst. To date, these self-healing polymers have been designed primarily for automotive paints, electronics, and aerospace applications [20].

The aim of this study is to encapsulate a clinically-approved tissue adhesive, 2-octylcyanoacrylate (OCA), in polyurethane (PU) microcapsules synthesized using *in situ* interfacial polymerization of toluene-2,4-diisocyanate (TDI) and polyethylene glycol 200 (PEG 200) through an oil-in-oil-in-water (o/o/w) microemulsion. During emulsification, microscopic

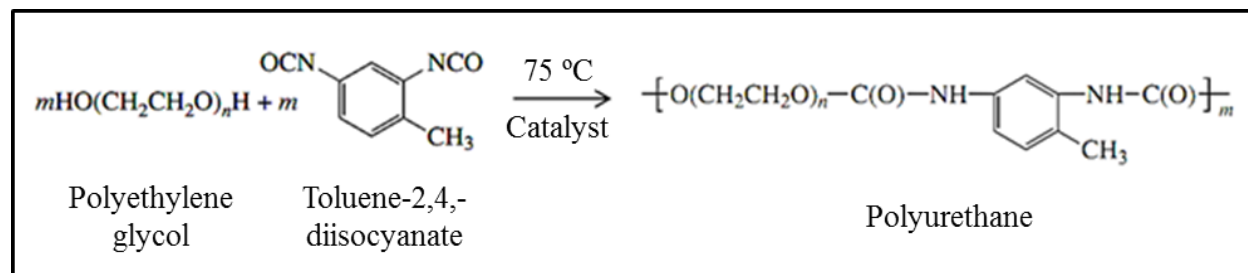
droplets containing an oil core are stabilized by surfactants and co-surfactants at the interface of two immiscible phases, which is followed by *in situ* interfacial polymerization where the meeting of reactant monomers at the interface results in the formation of a polymeric shell [21]. The PU microcapsule surface morphology, shell thickness, size, core OCA viability, thermal properties, and chemical structure were evaluated.

EXPERIMENTAL DETAILS

Reagent-grade TDI, PEG 200, paraffin oil, acetonitrile, bismuth neodecanoate (BNDC), 1,4-butanediol (1,4-BD), polyvinyl alcohol (PVA), polyethylene glycol sorbitan monolaurate (Tween 20), and sorbitane trioleate (Span 85) were all purchased from Sigma-Aldrich and used as received. OCA and D&C Violet used to stain the OCA were kindly donated by Ethicon, Inc., Raleigh, NC.

Polycondensation reaction

A polyurethane shell was synthesized via an *in situ* interfacial polymerization method using the monomers TDI and PEG 200 and a chain extender 1,4-BD [22,23]; the reaction is represented in Equation 1 [24]. Initially, the TDI dissolved in the organic phase was dispersed in the continuous aqueous phase containing a surfactant to form an oil-in-water (o/w) microemulsion under continuous agitation. PEG 200 present in the continuous aqueous phase comes in contact with the TDI in organic phase, initiating the polycondensation reaction between the TDI and PEG 200 monomers. The molar ratio of polyol and diisocyanate added was 1:2 and the chain extender 1,4 BD was added to complete the polymerization. The reaction progressed at the o/w interface for 2 h at 75 °C in the presence of a catalyst and resulted in the formation of a polymer layer at the interface.



Equation 1: Interfacial reaction that results in the formation of a polyurethane shell

Synthesis of microcapsules

The organic phase was divided into two sub-phases, A and B. Sub-phase A was formed by mixing OCA (1.5 mL) and paraffin oil (500 μL) while sub-phase B consisted of TDI (1 g) and the catalyst BNDC (300 μL) dissolved in acetonitrile (5 mL) containing Span 85 (50 μL) as a surfactant. The aqueous phase consisted of the cosurfactants PVA (1.5 g) and Tween 20 (500

μL), and PEG (1 mL) dissolved in deionized water (100 mL) using a VWR PowerMax Elite Dual-Speed Mixer. Sub-phase A was dispersed in sub-phase B and the resulting emulsion was then added to the aqueous phase under agitation to form an o/o/w microemulsion. The pH of the system was adjusted to 4 by adding 4M HCl (20 μL). The initial temperature of the system was maintained at 30 °C. After the addition of the organic phase, the temperature was increased to 50°C and maintained for 30 min. At this point, 1,4-BD (1 mL) was added to the system and the temperature was gradually increased to 70°C. The reaction was continued for 1.5 h at 450 rpm and then the agitation was turned off. The microcapsules were rinsed with deionized water, vacuum filtered, and air dried for 48 h (Figure 2). The reagents used were selected for this work based on their biocompatibility relative to alternative materials; for example, BNDC was selected as opposed to other heavy metal-based alternatives to minimize toxicity. OCA, PU, paraffin oil, and the surfactants selected are already FDA-approved or are mild detergents commonly used in *in vitro* studies. However, detailed *in vitro* analyses will be required to determine the biocompatibility of a self-healing PMMA formulation when compared with commercially-available systems.

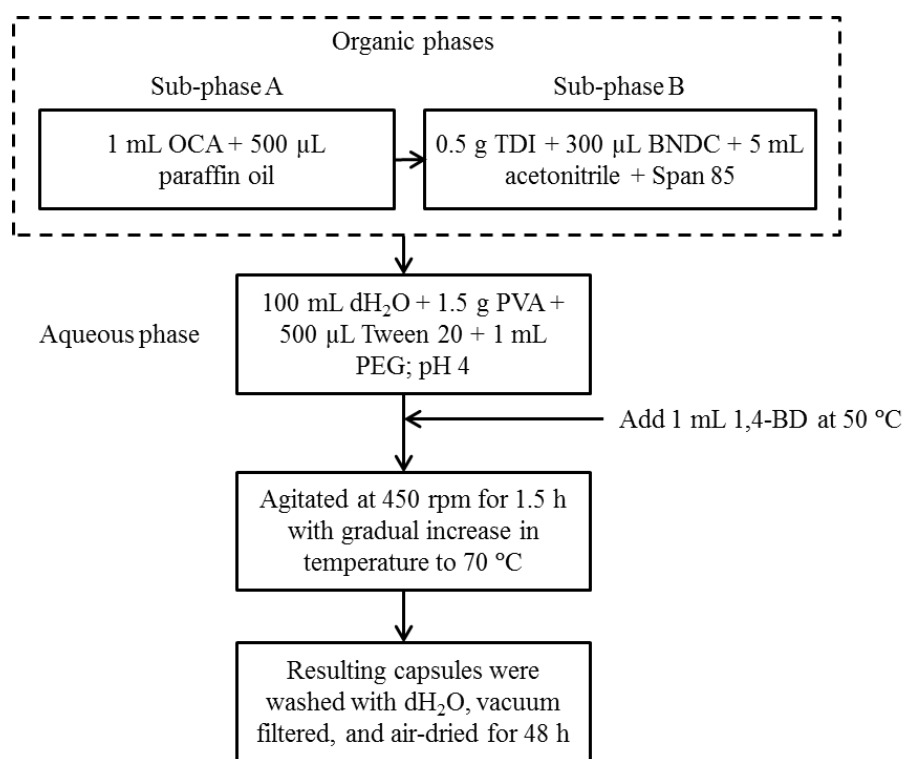


Figure 2: Schematic representation of microencapsulation process

Characterization techniques

Surface morphology, shell thickness, and size of the microcapsules were examined using scanning electron microscopy (SEM, FEI XL30 FEG-SEM). Microcapsules were mounted on a conductive stage using double sided carbon tape and were coated with a thin layer of gold/palladium using a vacuum sputter coater (Denton Desk IV). The voltage used for imaging

was 1.5 kV. The presence of encapsulated core material was studied by slicing capsules open under a stereoscopic microscope (Bausch & Lomb) with a scalpel blade. Fourier transform infrared spectroscopy (FT-IR, Thermo Electron Nicolet 8700) was performed to determine the chemical structure of the microcapsule shell formed by *in situ* polymerization. The obtained spectra were then compared with the standard FT-IR spectra of PU. The capsules used for this analysis were crushed into a pellet (Thermo Scientific KBr table press and 3 mm Die set) and then analyzed under reflecting mode to obtain transmission spectra of the polymer. Thermogravimetric analysis (TGA, TA Instruments Q500 V6.7) was carried out to determine the thermal degradation properties of microcapsules. The initial sample weight was kept within 10-11 mg. Samples were placed in a platinum sample pan and heated from 100°-600°C under nitrogen atmosphere at a linear heating increase of 10°C/min.

DISCUSSION

Surface and shell morphology

Microcapsules containing OCA were analyzed via SEM and are presented in Figure 3. Smooth-surfaced microcapsules with an average diameter of $299 \pm 110 \mu\text{m}$ and shell thickness of $26 \pm 5.2 \mu\text{m}$ (numbers given as average \pm standard deviation) were obtained (Figures 3A and 3B). The dark region surrounding the broken microcapsules indicates the presence of encapsulated core liquid (Figure 3C).

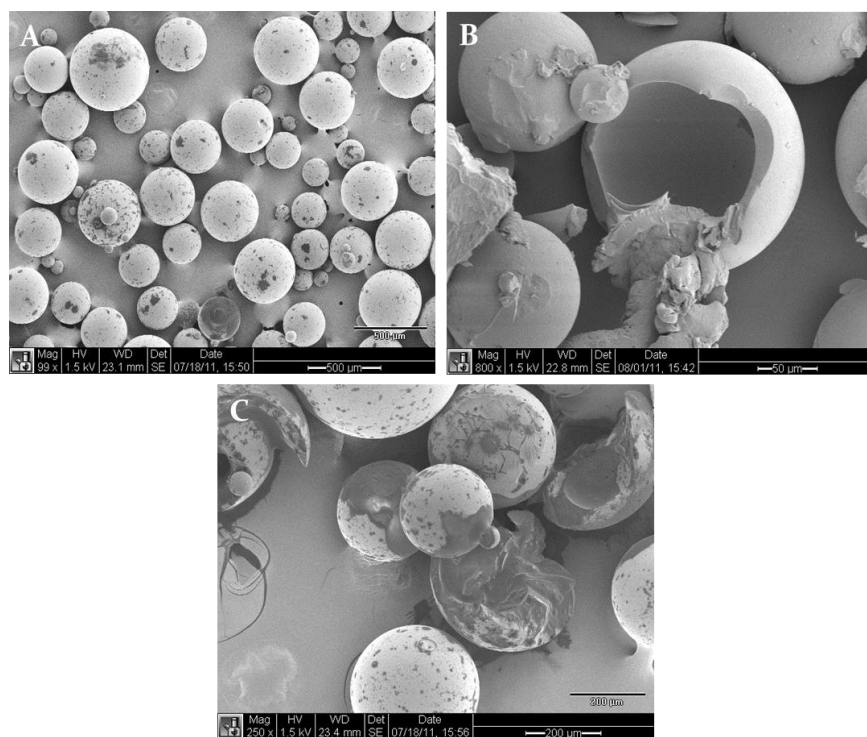


Figure 3: Surface and structural morphology of microcapsules. SEM images show (A) smooth shell morphology (B) capsule shell thickness, and (C) the presence of liquid content

Encapsulated core liquid viability test

Microcapsules containing dyed OCA were imaged under a stereoscopic microscope using a 5X digital zoom camera (Figure 4A). The presence of core liquid was observed by slicing open the microcapsules using a scalpel blade. A video was recorded during the experiment during which the release of the liquid core was clearly observed. A still shot of the video is shown in Figure 4B. The viability of encapsulated OCA was assessed by crushing a small amount of microcapsules between two cover slips. The released liquid content strongly glued the slides together (Figure 4C). OCA release was visualized from capsules of varying sizes within the reported diameter range although future optimizations will determine which agitation rate should be used to narrow the distribution of capsule sizes to improve population uniformity.

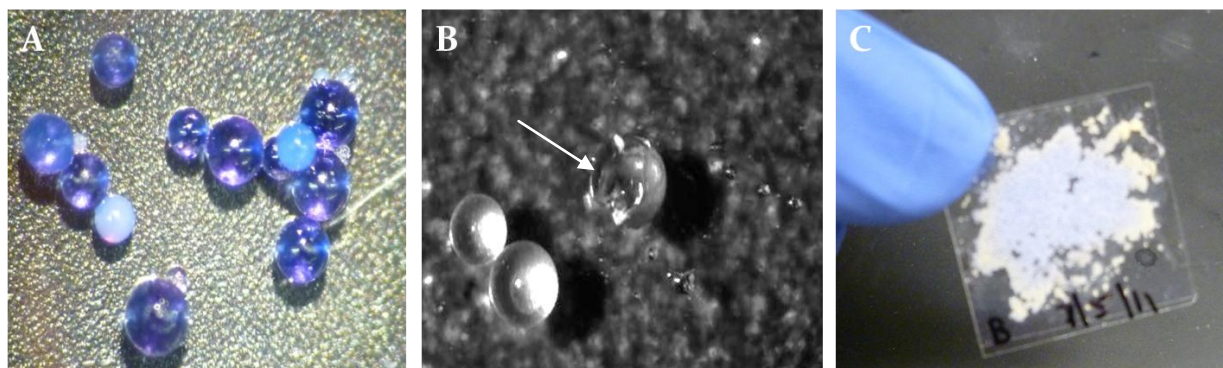


Figure 4: Assessment of encapsulated liquid contents (A) stereoscopic microscope image of microcapsules containing dyed OCA, (B) core liquid flowing out of the ruptured microcapsules, and (C) cover slips glued together by contents released from crushed microcapsules

Shell chemical structure analysis via FT-IR

FT-IR analysis of microcapsules was performed to verify the presence of PU chemical bonds along the polymer chain following the interfacial polymerization of PEG and TDI. As seen in Figure 5A, the spectrum contains an absorption band for N-H stretching at 3360 cm^{-1} and a bond representing CH_2 and CH_3 stretching at 2930 . C=O stretching of the urethane is observed at 1740 and 1690 cm^{-1} . Moreover, =C-H stretching at 2860 cm^{-1} , C-C stretching at 1530 cm^{-1} , C-O-C stretching at 1170 cm^{-1} , and =CH-H OOP bending of the phenyl at 818 cm^{-1} are also seen. These FT-IR results confirmed that shell of microcapsules is composed mainly of polyurethane [25-27].

Although the reaction between PEG and TDI is rapid in the presence of a catalyst, a longer reaction time is needed for total consumption of TDI monomer and complete polymerization of the PU shell. As seen in Figure 5B, FT-IR spectra of microcapsules synthesized with only 1 h reaction time contain an absorption band at 2276 cm^{-1} , indicating the presence of unreacted isocyanate group, $-\text{N}=\text{C}=\text{O}$ [25,28]. From the disappearance of the isocyanate band at 2276 cm^{-1} in Figure 5A when compared with Figure 5B, it can be inferred that

the TDI and PEG reactant monomers require a minimum of 2 h reaction time to form a completely synthesized PU shell.

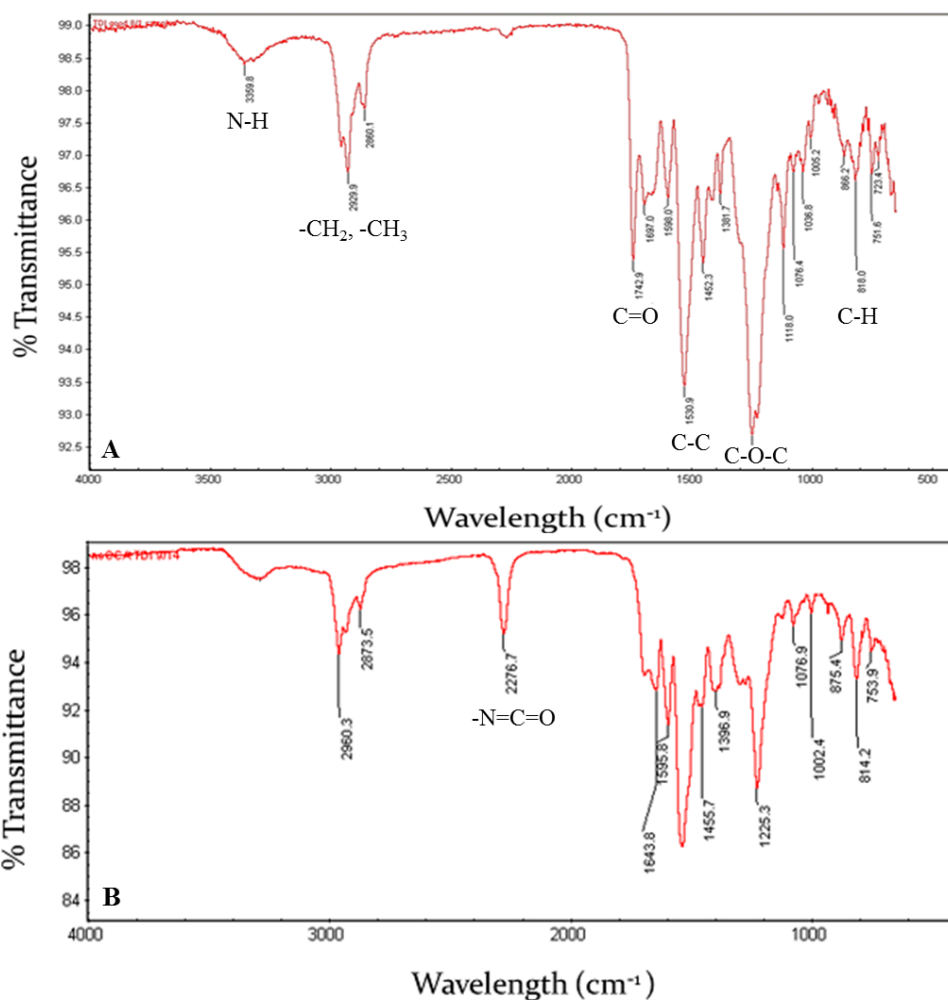


Figure 5: FT-IR spectra of hollow PU microcapsules (not containing OCA) prepared with TDI and PEG via interfacial polymerization following reaction times of (A) 2 h and (B) 1 h

Thermal analysis of microcapsules

The thermal degradation characteristics of the pure monomer OCA, pure PU shell, and PU microcapsules containing OCA were analyzed using TGA (Figures 6A and B). The percentage weight loss of the samples were attributed to the respective components according to the TGA analysis of PU microcapsules given by Li *et al.* [29]. As shown in Figure 6A, the TGA curve of OCA displays one step weight loss of 94% from 141° to 237°C. This rate of weight loss peaks at 233°C with complete vaporization by 242°C (Figure 6B). The TGA curve of the pure PU shell sample exhibits three phases of weight loss with increasing temperature. An initial weight loss of 4% from 48° to 147°C is attributed to adsorbed water evaporation. The second phase of weight loss of 67% from 130° to 305°C is due to degradation of the 1,4-BD-based soft segment

during the depolycondensation of PU; a maximal rate of weight loss is attained at 234°C. The third phase of weight loss of 23% from 305° to 544°C is attributed to the loss of the TDI-based hard segment in the polymer chain; 6% of the original sample weight remains at 643°C.

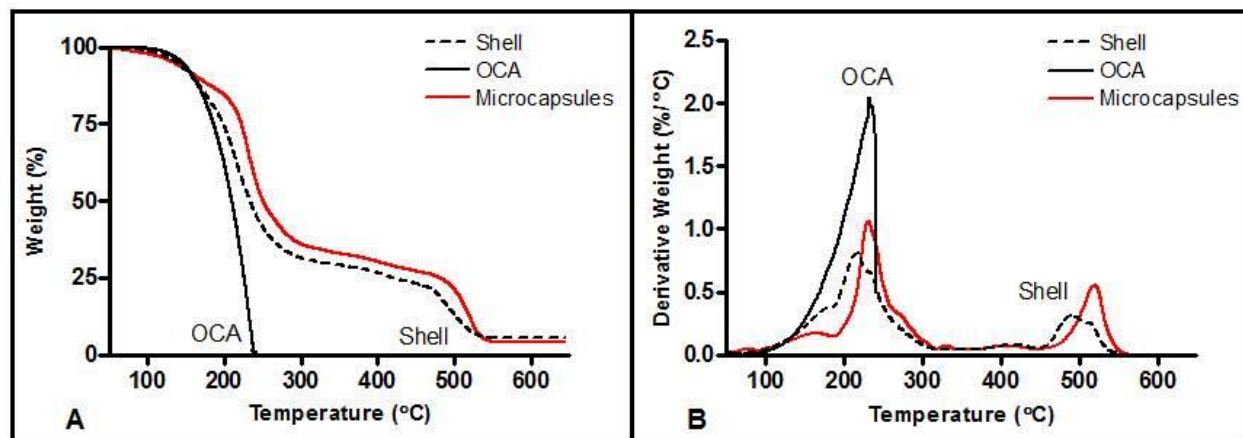


Figure 6: (A) TGA and (B) derivative TGA thermograms of OCA, PU shell, and microcapsules

The thermal degradation curves of PU microcapsules containing OCA are a combination of the TGA curves of pure OCA and pure PU shell samples. The TGA curves of microcapsules also show three phases of weight loss. The first phase of 6% weight loss was seen from 48° to 147°C and is attributed to the evaporation of residual water. The second phase of weight loss is from 152° to 326°C with 59% weight loss and a maximum rate of weight loss occurring at 230°C. The third phase is between 327° and 544°C with 31% of weight loss and 4% of the original sample weight remains at 643°C. The TGA data suggest the thermal stability of PU microcapsules containing OCA is improved over the pure materials, as the onset of degradation was at 148°C compared to pure OCA and PU, which began degrading at 141°C and 130°C, respectively.

Effect of pH on OCA stabilization

The optimization of the system pH plays a major role in stabilization of OCA with the continuous aqueous phase. The OCA monomer polymerizes rapidly in the presence of moisture, forming long chains of poly-alkyl cyanoacrylate [30]. In general, the OCA monomer is stabilized by a weak acid; to initiate the polymerization reaction, the weak acid must be neutralized by a weak base. A small amount of water is sufficient to initiate its anionic polymerization reaction; hence, maintaining an acidic environment during the encapsulation process can prevent OCA polymerization.

In this study, the microencapsulation of OCA was performed at various pH levels and it was found that a pH of 3-4 enables the encapsulation of OCA as an unreacted liquid monomer (Figure 7A). During the encapsulation process, the addition of the organic phase at pH >5 resulted in the formation of white soft microstructures that were seen in the reaction vessel after 10 min (Figures 7B and C). These microstructures could be formed due to the rapid

polymerization of OCA when it comes in contact with the moisture and/or polyol groups present in aqueous phase. The acidic environment at pH 4 decreased the OCA polymerization rate, resulting in the encapsulation of OCA.

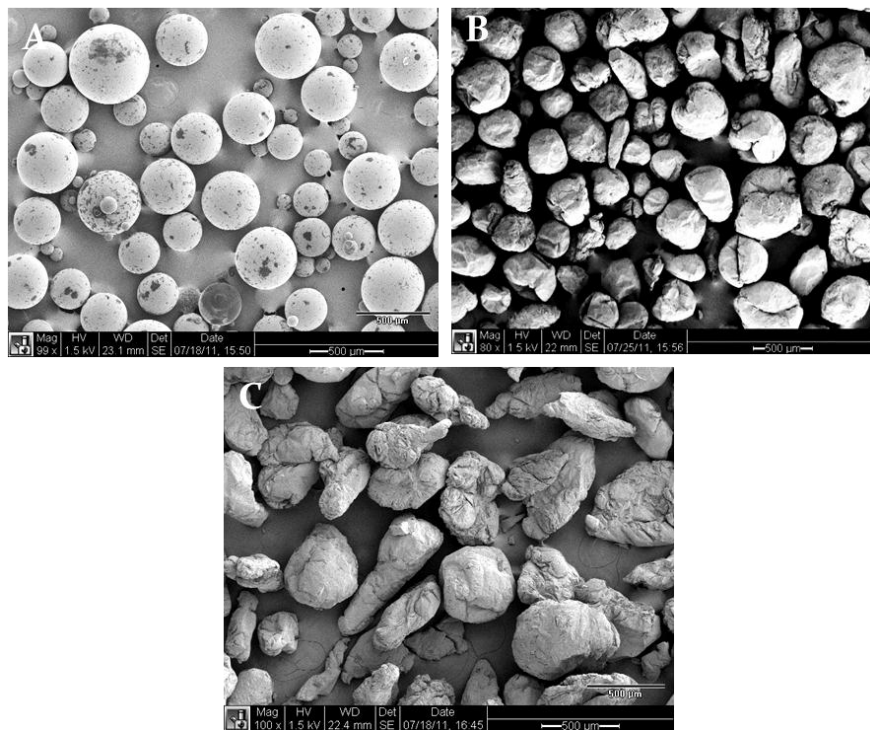


Figure 7: SEM images of microcapsules synthesized under various pH conditions (A) pH=4, (B) pH= 6, and (C) pH= 8

CONCLUSIONS

PU microcapsules containing liquid OCA were successfully synthesized using *in situ* interfacial polymerization of TDI and PEG 200 in an *o/o/w* microemulsion. Spherical microcapsules of an average diameter of $299 \pm 110 \mu\text{m}$ and shell thickness of $26 \pm 5.2 \mu\text{m}$ were fabricated with an agitation rate of 450 rpm. The presence and viability of encapsulated OCA was analyzed using a stereoscopic microscope and a slides adhering assay. In this study, a new encapsulation procedure was demonstrated using two immiscible solvents in the dispersed organic phase for encapsulating materials that are not compatible with classical *w/o* or *o/w* emulsions. The PU shell formation and completion of polycondensation reaction of TDI and PEG were confirmed by FT-IR analysis. Improved thermal properties of the microcapsules compared to empty PU microcapsules were observed by thermal analysis using TGA. Future work should include testing the shelf life of the OCA-filled microcapsules using TGA analysis and determining the capsule mechanical properties by individual capsule compression studies to determine the elastic stiffness of the shell wall and the strength of microcapsule shell [31]. The effects of agitation rate on microcapsule size and encapsulation efficiency should also be analyzed to determine the appropriate capsule content to release clinically-relevant volumes of

healing agent. Moreover, future investigations should focus on testing the mechanical properties and healing efficiency of these microcapsules embedded in a commercial PMMA bone cement matrix.

ACKNOWLEDGMENTS

This research was supported by an NIH NRSA Predoctoral Fellowship T32-GM8555 (ABWB) and NIH R21 EB 013874-01 (WMR). The authors would like to acknowledge Ethicon, Inc. for their generous donation of supplies and providing access to their equipment, and also Errol Purkett from Ethicon, Inc. for assisting in TGA usage. The authors would also like to thank Dr. Bruce Klitzman and Dr. Charles Wallace for their time and valuable feedback throughout the project.

REFERENCES

1. Kindt-Larsen, T., D.B. Smith, and J.S. Jensen, *Innovations in acrylic bone cement and application equipment*. Journal of Applied Biomaterials, 1995. **6**(1): p. 75-83.
2. Jasty, M., W.J. Maloney, C.R. Bragdon, D.O. O'Connor, T. Haire, and W.H. Harris, *The initiation of failure in cemented femoral components of hip arthroplasties*. Journal of Bone and Joint Surgery, British Volume, 1991. **73-B**(4): p. 551-558.
3. Culleton, T.P., P.J. Prendergast, and D. Taylor, *Fatigue failure in the cement mantle of an artificial hip joint*. Clinical Materials, 1993. **12**(2): p. 95-102.
4. Topoleski, L.D.T., P. Ducheyne, and J.M. Cuckler, *Microstructural pathway of fracture in poly(methyl methacrylate) bone cement*. Biomaterials, 1993. **14**(15): p. 1165-1172.
5. Huiskes, R., *Failed innovation in total hip replacement: Diagnosis and proposals for a cure*. Acta Orthopaedica, 1993. **64**(6): p. 699-716.
6. Saha, S. and S. Pal, *Mechanical properties of bone cement: A review*. Journal of Biomedical Materials Research, 1984. **18**(4): p. 435-462.
7. Murphy, B.P. and P.J. Prendergast, *Measurement of non-linear microcrack accumulation rates in polymethylmethacrylate bone cement under cyclic loading*. Journal of Materials Science: Materials in Medicine, 1999. **10**(12): p. 779-781.
8. Deb, S. and B. Vazquez, *The effect of cross-linking agents on acrylic bone cements containing radiopacifiers*. Biomaterials, 2001. **22**(15): p. 2177-2181.
9. Nien, Y.-H. and J. Chen, *Studies of the mechanical and thermal properties of cross-linked poly(methylmethacrylate-acrylic acid-allylmethacrylate)-modified bone cement*. Journal of Applied Polymer Science, 2006. **100**(5): p. 3727-3732.
10. Muraikami, A., J.C. Behiri, and W. Bonfield, *Rubber-modified bone cement*. Journal of Materials Science, 1988. **23**(6): p. 2029-2036.
11. Yang, J.-M., C.-S. Lu, Y.-G. Hsu, and C.-H. Shih, *Mechanical properties of acrylic bone cement containing PMMA-SiO₂ hybrid sol-gel material*. Journal of Biomedical Materials Research, 1997. **38**(2): p. 143-154.
12. Taitsman, J.P. and S. Saha, *Tensile strength of wire-reinforced bone cement and twisted stainless-steel wire*. The Journal of Bone and Joint Surgery, 1977. **59**(3): p. 419-425.

13. Brochu, A.B.W., S.L. Craig, and W.M. Reichert, *Self-healing biomaterials*. Journal of Biomedical Materials Research Part A, 2011. **96A**(2): p. 492-506.
14. White, S.R., N.R. Sottos, P.H. Geubelle, J.S. Moore, M.R. Kessler, S.R. Sriram, E.N. Brown, and S. Viswanathan, *Autonomic healing of polymer composites*. Nature, 2001. **409**(6822): p. 794-797.
15. Sottos, N., S. White, and I. Bond, *Introduction: self-healing polymers and composites*. Journal of The Royal Society, Interface, 2007. **4**(13): p. 347-348.
16. Risch Sara, J., *Encapsulation: Overview of Uses and Techniques*, in *Encapsulation and Controlled Release of Food Ingredients*. 1995, American Chemical Society. p. 2-7.
17. Deasy, P.B., *Microencapsulation and related drug processes*. Marcel Dekker, 1984.
18. Luo, W.-j., W. Yang, S. Jiang, J.-m. Feng, and M.-b. Yang, *Microencapsulation of decabromodiphenyl ether by in situ polymerization: Preparation and characterization*. Polymer Degradation and Stability, 2007. **92**(7): p. 1359-1364.
19. Yuan, Y.C., M.Z. Rong, and M.Q. Zhang. *Preparation and characterization of microencapsulated polythiol*. Polymer, 2008. **49**(10): p.2531-2541.
20. Kessler, M.R., *Self-healing: A new paradigm in materials design*. Proceedings of the Institution of Mechanical Engineers, Part G: Journal of Aerospace Engineering, 2007. **221**(4): p. 479-495.
21. Magdassi, S. and E. Touitou, *Novel cosmetic delivery systems*. Marcel Dekker, 1999.
22. Ramanathan L.S, P.G. Shukula, and S. Sivaram, *Synthesis and characterization of polyurethane microspheres* Pure and applied chemistry, 1998. **70**(6): p.1295-1299.
23. Iskakov, R., E.O. Batyrbekov, M.B. Leonova, and B.A. Zhubanov, *Preparation and release profiles of cyclophosphamide from segmented polyurethanes*. Journal of Applied Polymer Science, 2000. **75**(1): p. 35-43.
24. Min, B.M., G. Lee, S.H. Kim, Y.S. Nam, T.S. Lee, and W.H. Park, *Electrospinning of silk fibroin nanofibers and its effect on the adhesion and spreading of normal human keratinocytes and fibroblasts in vitro*. Biomaterials, 2004. **25**(7-8): p. 1289-1297.
25. Bouchemal, K., S. Briancon, E. Perrier, H. Fessi, I. Bonnet, and N. Zydowicz, *Synthesis and characterization of polyurethane and poly(ether urethane) nanocapsules using a new technique of interfacial polycondensation combined to spontaneous emulsification*. International Journal of Pharmaceutics, 2004. **269**(1): p. 89-100.
26. Hong, K. and S. Park, *Preparation of polyurethane microcapsules with different soft segments and their characteristics*. Reactive and Functional Polymers, 1999. **42**(3): p. 193-200.
27. Su, J.-F., L.-X. Wang, L. Ren, Z. Huang, and X.-W. Meng, *Preparation and characterization of polyurethane microcapsules containing n-octadecane with styrene-maleic anhydride as a surfactant by interfacial polycondensation*. Journal of Applied Polymer Science, 2006. **102**(5): p. 4996-5006.
28. Lan, X.-Z., Z.-C. Tan, G.-L. Zou, L.-X. Sun, and T. Zhang, *Microencapsulation of n-Eicosane as Energy Storage Material*. Chinese Journal of Chemistry, 2004. **22**(5): p. 411-414.
29. Li, Y. and Z. Cai, *Microencapsulation and application of fluorine-free water repellent agent-AH102*. Journal of Applied Polymer Science, 2011. **119**(1): p. 330-335.
30. Dossi, M., G. Storti, and D. Moscatelli, *Synthesis of Poly(Alkyl Cyanoacrylates) as Biodegradable Polymers for Drug Delivery Applications*. Macromolecular Symposia, 2010. **289**(1): p. 124-128.

31. Yang, J., M.W. Keller, J.S. Moore, S.R. White, and N.R. Sottos, *Microencapsulation of Isocyanates for Self-Healing Polymers*. *Macromolecules*, 2008. **41**(24): p. 9650-9655.